IRSTI 29.19.22

Myasnikova L.N.[1], Istlyaup A.S.[1], Sergeyev D.M.[1,2]

[1]Zhubanov Aktobe Regional State University,
Kazakhstan, Aktobe, e-mail: myasnikova_ln@mail.ru
[2]Begeldinov Military Institute of Air Defence Forces,
Kazakhstan, Aktobe

COMPUTER SIMULATION OF THE DENSITY OF THE STATE OF THE NAF NANOCRYSTAL

At present, various theoretical research methods are intensively used to interpret experimental results related to the study of the properties of defects in solids. Progress in this direction is possible thanks to the improvement of computer technology and the development of modern quantum chemical packages. The paper presents the results of computer simulation of the density of states and the total energy of an ideal NaF nanocrystal ($Na_{13}F_{14}$, Na_4F_5, $Na_{22}F_{23}$) and with the simplest point defects in various cluster compounds ($Na_{12}F_{13}$, $Na_{21}F_{22}$). Simulation of characteristics is implemented in the Atomistix ToolKit with Virtual NanoLab program in GGA (generalized gradient approximation) functionality. Objects studied are quantum dots. The results obtained may be useful in the study of nanocrystals.

Key word: NaF nanocrystal, density of states, band structure, total energy, computer simulation.

Мясникова Л.Н.[1], Истляуп А.С.[1], СергеевД.М.[1,2]

[1]Қ. Жұбанов атындағы Ақтөбе өңірлік мемлекеттік университеті,
Қазақстан, Ақтөбе қ., e-mail: myasnikova_ln@mail.ru
[2]Т. Бигельдинов атындағы Әуе қорғанысы күштерінің Әскери институты,
Қазақстан, Ақтөбе қ.

NaF нанокристалының күй тығыздығын компьютерлік модельдеу

Қазіргі кезде қатты денелердегі ақаулардың қасиеттерін зерттеуге байланысты эксперименталды нәтижелерді түсіндіру үшін түрлі теориялық зерттеулер әдісі белсенді қолданылады. Бұл бағыттағы прогресс компьютерлік технологияны жетілдіру және заманауи кванттық химиялық жиынтықтарды әзірлеу арқасында мүмкін болады. Берілген жұмыста NaF ($Na_{13}F_{14}$, Na_4F_5, $Na_{22}F_{23}$) идеал нанокристалы мен қарапайым нүктелік ақаулары бар түрлі кластерлік қосылыстардың ($Na_{12}F_{13}$, $Na_{21}F_{22}$) күй тығыздығы мен толық энергиясының компьютерлік модельдеуі көрсетілген. Сипаттамалардың модельденуі Atomistix ToolKit with Virtual NanoLab бағдарламасы негізінде GGA (generalized gradient approximation) функционалдылығында жүзеге асырылды. Зерттелген объектілер кванттық нүктелерге жатқызылады. Алынған нәтижелерді нанокристалдарды зерттеуде пайдалы болуы мүмкін.

Түйін сөздер: NaF нанокристалы, күй тығыздығы, зоналық құрылыс, толық энергия, компьютерлік модельдеу.

Мясникова Л.Н.[1], Истляуп А.С.[1], СергеевД.М.[1,2]

[1]Актюбинский региональный государственный университет им. К. Жубанова,
Казахстан, г. Актобе, e-mail: myasnikova_ln@mail.ru
[2]Военный институт Сил воздушной обороны им. Т.Я. Бегельдинова,
Казахстан, г. Актобе

Компьютерное моделирование плотности состояния нанокристалла NaF

В настоящее время интенсивно применяются различные теоретические методы исследования для интерпретации экспериментальных результатов, связанных с изучением свойств дефектов в твердых телах. Прогресс в этом направлении возможен благодаря совершенствованию компьютерных технологий и разработке современных квантово-химических пакетов. В работе представлены результаты компьютерного моделирования плотности состояний и полной энергии идеального нанокристалла NaF ($Na_{13}F_{14}$, Na_4F_5, $Na_{22}F_{23}$) и с простейшими точечными дефектами в различных кластерных соединениях ($Na_{12}F_{13}$, $Na_{21}F_{22}$). Моделирование характеристик реализовано в программе Atomistix ToolKit with Virtual NanoLab в функциональности GGA (generalized gradient approximation). Исследуемые объекты относятся к квантовым точкам. Полученные результаты могут быть полезными при исследовании нанокристаллов.

Ключевые слова: нанокристалл NaF, плотность состояний, зонная структура, полная энергия, компьютерное моделирование.

Introduction

Currently, the properties of alkali halide nanocrystals are of great technological interest on the part of specialists in chemistry, physics, and also engineers [1-7]. In [8], the results on adhesion, bonding and construction, surface electron states and other subtle effects in nano-lattices were demonstrated. The processes of demetallization of alkali halide clusters by shock-induced fragmentation of cubic $Na_{14}F_{12}$ are discussed in detail in [9]. The reactions arising during collisions of NaF clusters with the silicon surface were investigated in [10]. The X-ray diffraction study of NaF nanocrystals in a photo-refractory glass is described in detail in [11]. In [12–15], the structural, electronic, dynamic, and thermodynamic properties of alkali metal halides were calculated from first principles using both full-potential and plane wave pseudopotential methods. The use of various effects, such as deformation, allows us to consider the new possibilities of using alkaline halide dosimetry crystals [16-18].

It is believed that nanostructured objects include such objects, the characteristic dimensions of which lie in the range from 1 to 100 nm. In general, this dimensional limit is somewhat conditional. The main feature of nanoobjects is that, because of their smallness, they exhibit special properties [19]. Since in nanocrystalline structures the main part of ions lies in the outer layer, many of their properties are revealed on their surface. In many cases, these special properties can manifest themselves even when the size of nanoobjects exceeds the conventionally set limit of 100 nm. In [20], the energy of a 2×2×2 cubic cell of a NaF crystal was calculated using the Hartree-Fock method.

A deep understanding of the optical properties of solids is impossible without a detailed knowledge of their energy electronic structure. Electronic processes in ionic crystals are considered on the basis of an approximate quantum-mechanical theory developed by Bloch, Wilson, and others, called the band theory. In the band theory, the motion of electrons and nuclei is divided within the framework of the Born-Oppenheimer adiabatic approximation.

One of the characteristics of the reflecting property of a nano-object is the electron density of states, which is an important parameter in statistical and solid state physics [21], which determines the number of energy levels in the energy interval per unit volume or area.

In this paper, an attempt was made using computer simulation using Atomistix ToolKit with Virtual NanoLab to determine the density of states, the total energy and the band structure of a NaF crystal in various “negative” cluster compounds ($Na_{13}F_{14}$, $Na_{12}F_{13}$, Na_4F_5, $Na_{22}F_{23}$, $Na_{21}F_{22}$) at 1 K .

Description of the object and methods of research

Isolated alkali metal atoms Na and F halide have the following electronic configuration: Na^0 –

$1s^2 2s^2 2p^6 3s^1$, F^0 – $1s^2 2s^2 2p^5$. In the NaF matrix, the ions of the corresponding elements take on the following electron configuration – Na^+ – $1s^2 2s^2 2p^6$, F^- – $1s^2 2s^2 2p^6$. As a result, the valence electron located on the outer shell of Na^0 completely goes to F^0.

The $Na_{13}F_{14}$ cluster contains 27 ions, as shown in Figure 1*a*, is a negatively charged cube with indices (*j*, *k*, *i*) = (3, 3, 3) and with O_h symmetry. The $Na_{12}F_{13}$ cluster is obtained by removing the Na^+ and F^- ions from the central region of the nanoobject (Figure 1*b*). The Na_4F_5 object contains 9 ions, as shown in Figure 1*c*, is a plane with indices (*j*, *k*, *i*) = (3, 3, 1). The $Na_{22}F_{23}$ cluster is a parallelepiped with indices (*j*, *k*, *i*) = (3, 3, 5), containing 45 ions (Figure 1*d*). The $Na_{21}F_{22}$ nanoobject, shown in Figure 1*f*, was obtained by removing Na^+ and F^- ions from the center of the penultimate layer [7]. The distance between the centers of the nearest ions in NaF is 2.31Å [22-23].

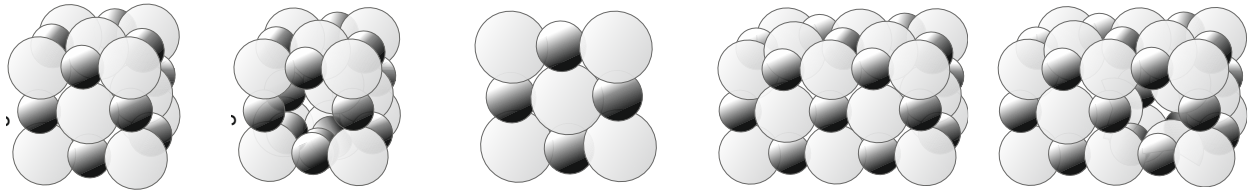

$Na_{13}F_{14}$ *a* $Na_{12}F_{13}$ *b* Na_4F_5 *c* $Na_{22}F_{23}$ *d* $Na_{21}F_{22}$ *f*

Figure 1 – The geometry of NaF clusters

In the adiabatic approximation, the solution of the Schrödinger equation shows that the states of an excess electron in a crystal with a periodic field are described by the Bloch wave functions

$$u_k(\vec{r})\exp\left\{-i\left(\frac{E}{h}t-\vec{k}\vec{r}\right)\right\},$$

where the function $u_k(\vec{r})$ has translational lattice symmetry, *E* is energy, $\vec{k}$ is the wave vector. For a face-centered alkali halide crystal, the first Brillouin zone is a fourteen-shaped truncated octahedron shape; six faces have the form of squares, eight – the form of regular hexagons. The Γ -point lies at the center of the first Brillouin zone (*k = 0*), the X-point lies at the center of the square plane, the L-point is at the center of the hexagon. Along the [100] axis, the wave vector value varies from 0 to k_x, along the [111] direction from 0 to k_L. In all alkali halide crystals, the maximum of the valence band and the minimum of the conduction band are located in the center of the Brillouin zone (point Γ). The upper hole zones are formed from the *p*-states of the halogen and have a negative dispersion typical of the *p*-zones. The bottom of the conduction band is *s*-character, the effective electron mass is isotropic and has a value of the order of $(0{,}5\text{-}1)m_0$.

Computer simulation of the objects of study was carried out within the framework of the density functional theory in the local density approximation.

When performing calculations, the exchange-correlation functional is approximated by a generalized gradient approximation (GGA):

$$E_{xc}^{GGA}[n]=\int n(\mathbf{r})\varepsilon^{GGA}\left(n(\mathbf{r}),\left|\Delta n(\mathbf{r})\right|\right)n(\mathbf{r})d\mathbf{r} \quad ,$$

Where $n(\mathbf{r})$ is the density of a non-degenerate ground state of a system of *N* electrons in a potential $v(\mathbf{r})$, corresponding to the ground state Ψ and energy *E*, ε^{GGA} is the universal functional GGA, $e_{xc}(n)$ is exchange-correlation energy of a homogeneous gas with a density *n*.

The main parameters of the computing resource are: Intel (R) Core (TM) i7-4790 CPU @ 3.6 GHz 8 core processor, 8 GB RAM, system type – 64-bit operating system, operating system – Windows 8.1.

The position of the electron is described by the wave function $\psi(x, y, z)$. The probability of finding

an electron at a certain point (x, y, z) is described by the expression $|\psi\ (x,\ y,\ z)|^2$, where the total probability $\int_{-\infty}^{\infty} |\psi\ (x, y, z)|^2 dxdydz$ is normalized to one.

Electrons at the bottom of the conduction band behave like free particles (with an effective mass) trapped in a box. Consider the electrons of the conduction band, but the result for holes is similar. For our parabolic conduction band:

$$(E - E_c) = \frac{\hbar^2 k^2}{2m^*}.$$

For electrons in a rectangular volume L_x through L_y through L_z with an infinite limiting potential U (x, y, z) = 0 inside the box and outside ∞), the electron wave function ψ should reach zero and take the form of a harmonic function inside the region. Wave function solution:

$$\psi\ (x, y, z) = \sin(k_x x)\sin(k_y y)\sin(k_z z),$$

where k_x, k_y и k_z are wave vectors for an electron in directions x, y and z. The real wave function in a solid is more complex and periodic (with a crystal lattice), but this is a good approximation for parabolic regions near the edges of the zone.

Fulfillment of boundary conditions: when x, y or z = 0, the sinusoidal functions vanish. On opposite boundaries of the rectangular region, *sin* (k_xL_x) = 0, *sin* (k_yL_y) = 0, and *sin* (k_zL_z) = 0,for directions x, y and z. Allowed wave vectors satisfy:

$$k_xL_x = \pi n_x,\ k_yL_y = \pi n_y,\ k_zL_z = \pi n_z,$$

where n_x, n_y, n_z are whole numbers [24].

Simulation results

Using computer simulation, the density spectra of the states of the NaF nanocrystal were obtained in various cluster compounds ($Na_{13}F_{14}$, $Na_{12}F_{13}$, Na_4F_5, $Na_{22}F_{23}$, $Na_{21}F_{22}$) at a temperature of 1 K (Figure 2). The total and specific energy is calculated not only in the indicated objects, but also in their "positive" twins (table 1).

In Figure 2, a certain amount of energy levels in the energy range from -20 eV to 20 eV are clearly visible. In this case, in all spectra (Fig. 2 *a* – *f*), the first pronounced narrow energy level is located in the region of –18 eV. The main relatively wide energy level is observed in the region -1.5 ÷ -2 eV to 0.5 eV. Then a series of narrow energy levels is recorded in the energy range from 3 eV to 16 ÷ 20 eV. The characteristic form of energy levels in the density spectra of states indicates that a NaF nanocrystal in various cluster compounds ($Na_{13}F_{14}$, $Na_{12}F_{13}$, Na_4F_5, $Na_{22}F_{23}$, $Na_{21}F_{22}$) at 1 K can be attributed to quantum dots.

Table 1 – Full and specific energy of NaF nanocrystal

Object	Total energy, eV	Specific energy, eV	Object	Total energy, eV	Specific energy, eV
$Na_{13}F_{14}$	-9140,61667	-338,5413581	$Na_{14}F_{13}$	- 8510,59120	-315,2070815
$Na_{12}F_{13}$	-8480,54235	-339,221694	$Na_{13}F_{12}$	- 7852,99247	-314,1196988
Na_4F_5	-3251,71604	-361,3017822	Na_5F_4	- 2620,11205	-291,1235611
$Na_{22}F_{23}$	-15030,90457	-334,0201016	$Na_{23}F_{22}$	- 14400,23120	-320,0051378
$Na_{21}F_{22}$	-14368,42587	-334,1494388	$Na_{22}F_{21}$	- 13742,51906	-319,5934665

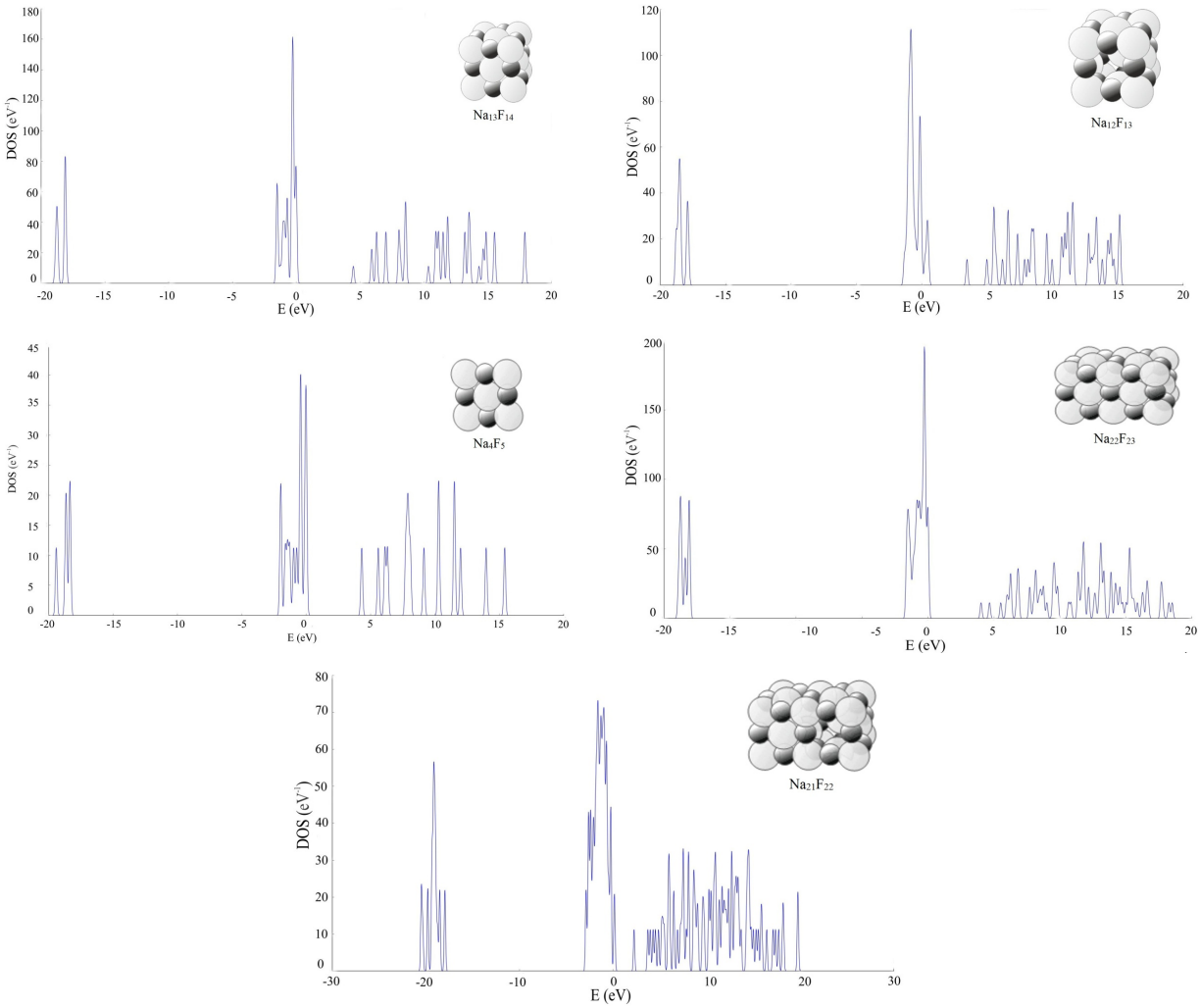

Figure 2 – Density of states of NaF nanocrystal in various cluster compounds ($Na_{13}F_{14}$, $Na_{12}F_{13}$, Na_4F_5, $Na_{22}F_{23}$, $Na_{21}F_{22}$)

When plotting the dependence of the total energy on the number of elements in the negatively charged clusters $Na_{13}F_{14}$, $Na_{12}F_{13}$, Na_4F_5, $Na_{22}F_{23}$, $Na_{21}F_{22}$, we observe that the points lie along a straight line (Figure 3). A similar qualitative result is obtained with positively charged clusters of $Na_{14}F_{13}$, $Na_{13}F_{12}$, Na_5F_4, $Na_{23}F_{22}$, $Na_{22}F_{21}$.

According to the table, the total energy in negatively charged clusters of $Na_{13}F_{14}$, $Na_{12}F_{13}$, Na_4F_5, $Na_{22}F_{23}$,$Na_{21}F_{22}$ varies from -3251.71604 eV to -15030.90457 eV. However, the specific energy for the $Na_{13}F_{14}$, $Na_{12}F_{13}$, $Na_{22}F_{23}$,$Na_{21}F_{22}$ clusters has a narrower interval in the region from –334.0201016 eV to -339.22161694 eV. At the same time, for the Na_4F_5 crystal, the specific energy is the smallest value of –361.3017822 eV.

The total energy in positively charged clusters of $Na_{14}F_{13}$, $Na_{13}F_{12}$, Na_5F_4, $Na_{23}F_{22}$, $Na_{22}F_{21}$ varies from -2620.11205 eV to -14400.23120 eV. However, the specific energy for $Na_{14}F_{13}$, $Na_{13}F_{12}$, $Na_{23}F_{22}$, $Na_{22}F_{21}$ clusters also has a narrow interval in the range from -314.1196988 eV to -320.0051378 eV. At the same time, for the Na_5F_4 crystal, the specific energy is the highest value of –291.1235611 eV.

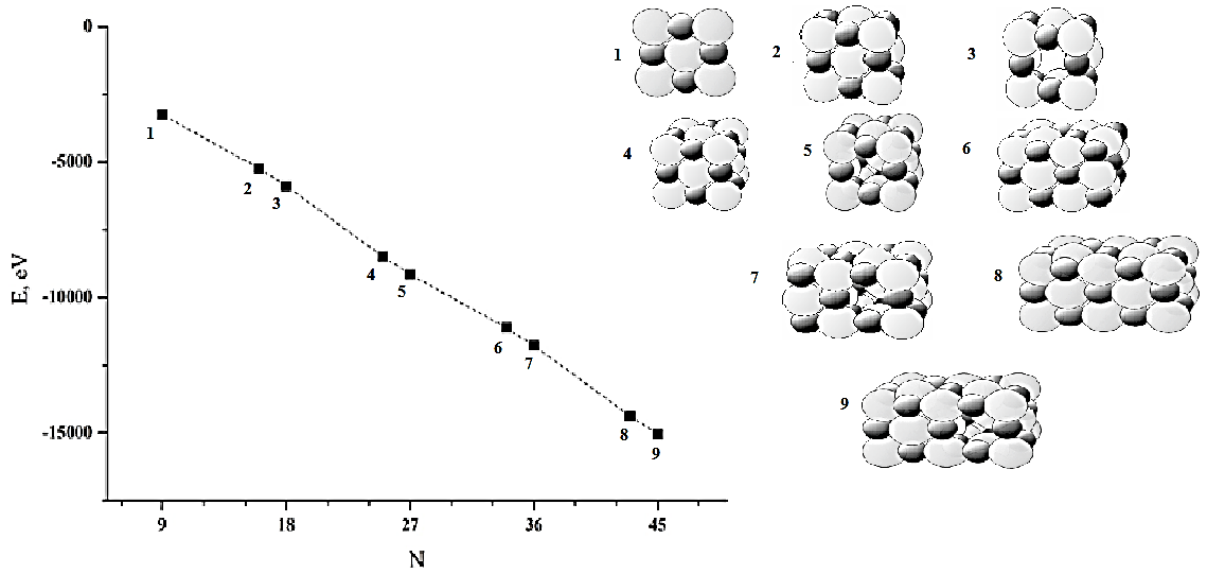

Figure 3 – Dependence of total energy on the number of elements in NaF clusters

Conclusion

Thus, in this work, in the framework of the density functional theory, the density of states and the total energy of the NaF nanocrystal are calculated, and the results of computer simulation of the band structure in various cluster compounds ($Na_{13}F_{14}$, $Na_{12}F_{13}$, Na_4F_5, $Na_{22}F_{23}$, $Na_{21}F_{22}$) are presented at a temperature of 1 K. Simulation of characteristics implemented in the program Atomistix ToolKit with Virtual NanoLab. The characteristic form of the density of states suggests that these objects can be attributed to quantum dots.

References

1 Lushchik Ch., Lushchik A. Evolution of Anion and Cation Excitons in Alkali Halide Crystals // Physics of the Solid State. – 2018. – Vol. 60. – P. 1487-1505.

2 Shunkeyev K., Sergeyev D., Myasnikova L., Barmina A., Shunkeyev S., Zhanturina N., Aimaganbetova Z. Vacancy dipole currents of thermostimulated depolarization in a plastically deformed KCl crystal // Russian Physics Journal. – 2014. – Vol. 57, №.4. – P.451-458.

3 Lushchik A., Lushchik Ch., Vasil'chenko E., Popov A.I. Radiation creation of cation defects in alkali halide crystals: Review and today's concept // Low Temperature Physics. – 2018. – Vol. 44. – No. 4. – P. 357-367.

4 Shunkeyev K., Zhanturina N., Aimaganbetova Z., Myasnikova L., Barmina A., Sagimbaeva Sh., Sergeyev D. Features of the action of an uniaxial deformation on the radiative annihilation of excitons in KBr crystal // Journal of Physics: Conf. Series. – 2018. – Vol. 1115. – 052010.

5 Shunkeyev K., Zhanturina N., Aimaganbetova Z., Barmina A., Myasnikova L., Sagymbaeva Sh., Sergeyev D. The specifics of radiative annihilation of self-trapped excitons in a KI-Tl crystal under low-temperature deformation // Low temperature physics. – 2016. – Vol. 42. – №7. – P. 580-583.

6 Toyozawa Y. Elementary processes in luminescence // J. of Luminescence. – 1976. – Vol. 12/13. – P. 13-21.

7 Mathews M.S., Amaechi B.T., Ramalingam K., Ccahuana-Vasquez R.A., Chedjieu I.P., Mackey A.C., Karlinsey R.L. In situ remineralisation of eroded enamel lesions by NaF rinses // Archives of oral biology. – 2012. – Vol. 57. – P. 525-530.

8 Robert L. Whetten. Alkali Halide Nanocrystals // Acc. Chem. Rev. – 1993. – Vol. 26. – P. 49-56.

9 Rainer D. Beck, Pamela St. John, Margie L. Homer, Robert L. Whetten. Demetallization of alkali/alkali-halide clusters: impact-induced fragmentation of cubic $Na_{14}F_{12}$ // Chemical physical letters. – 1991. – Vol. 187. – N 1,2. – P. 122-128.

10 Pamela M. St. John, Rainer D. Beck, Robert L. Whetten. Reactions in Cluster-Surface Collisions // Physical review letters. – 1992. – Vol. 69. – N 9. – P. 1467-1470.

11 Lumeau J., Chamma K., Glebova L., Glebov L. X-ray diffraction study of NaF nano-crystals in photo-thermo-refractive glass // Journal of Non-Crystalline Solids. – 2014. – Vol. 405. – P. 188–195.

12 Messaoudi I.S., Zaoui A., Ferhat M. Band-gap and phonon distribution in alkali halides // Phys. Status Solidi B. – 2014. – P. 1-6.

13 Mamula B.P., Kuzmanović B., Ilić M.M., Ivanović N., Novaković N., Bonding mechanism of some simple ionic systems: Bader topological analysis of some alkali halides and hydrides revisited // Physica B: Condensed Matter. – 2018. – Vol. 545. – P. 146-151.

14 Cui He, Cui-E Hu, Tian Zhang, Yuan-Yuan Qi, Xiang-Rong Chen. Lattice dynamics and thermal conductivity of cesium chloride via first-principles investigation // Solid State Communications. – 2017. – Vol. 254. – P. 31-36.

15 Ting Liang, Wen-Qi Chen, Cui-E. Hu, Xiang-Rong Chen, Qi-Feng Chen. Lattice dynamics and thermal conductivity of lithium fluoride via first-principles calculations // Solid State Communications. – 2018. – Vol. 272. – P. 28-32.

16 Chandra B.P., Chandra V.K., Jha Piyush, Patel R.P., Baghel R.N. Possibility of elastico-mechanoluminescence dosimetry using alkali halides and other crystals // Radiation Measurements. – 2015. – Vol. 78. – P. 9-16.

17 Chandra B.P. Mechanoluminescence induced by elastic deformation of coloured alkali halide crystals using pressure steps // Journal of Luminescence. – 2008. – Vol. 128. – P. 1217–1224.

18 Kucharczyk W. Photoelastic effect and density derivative of the refractive index in alkali halides // Journal of Physics and Chemistry of Solids. – 1989. – Vol. 50(7). – P. 709-712.

19 Bryukvina L., Ivanov N., Nebogin S. Relationships between lithium and sodium nanoparticles and color centers formation in LiF and NaF crystals with hydroxide and magnesium ions impurities // Journal of Physics and Chemistry of Solids. – 2018. – Vol. 120. – P. 133-139.

20 Pandey R., Yang X., Vail J.M., Zuo J. Derivation of Pair Potentials from First Principles and Simulation of NaF Clusters // Solid State Communications. – 1992. – Vol. 81(7). – P. 549-552.

21 Landman U., Scharf D., Jortner J. Electron Localization in Alkali-Halide Clusters // Physical review letters. – 1985. – Vol. 54. – N. 16. – P. 1860-1863.

22 Hoya J., Laborde J.I., Richard D., Rentería M. Ab initio study of F-centers in alkali halides // Computational Materials Science. – 2017. – Vol. 139. – P. 1-7.

23 Kong D., Dong C., Wei X., Man C., Lei X., Mao F., Li X. Size matching effect between anion vacancies and halide ions in passive film breakdown on copper // Electrochimica Acta. – 2018. – Vol. 292. – P. 817-827.

24 Jackson K.A. Local Spin Density Treatment of Substitutional Defects in Ionic Crystals with Self-Interaction Corrections // Advances in Atomic, Molecular, and Optical Physics. – 2015. – Vol. 64. – P. 15-27.

25 Myasnikova A., Mysovskya A., Paklin A., Shalaev A. Structure and optical properties of copper impurity in LiF and NaF crystals from ab initio calculations // Chemical Physics Letters. – 2015. – Vol. 633. – P. 218-222.

References

1 Ch. Lushchik and A. Lushchik, Physics of the Solid State **60**, 1487-1505 (2018).

2 K. Shunkeyev, D. Sergeyev, L. Myasnikova, A. Barmina, S. Shunkeyev, N. Zhanturina and Z. Aimaganbetova, Russian Physics Journal **57**, 451-458 (2014).

a. Lushchik, Ch. Lushchik, E. Vasil'chenko and A.I. Popov, Low Temperature Physics, **44**, 357-367 (2018).

3 K. Shunkeyev, N. Zhanturina, Z. Aimaganbetova, L. Myasnikova, A. Barmina, Sh. Sagimbaeva and D. Sergeyev, Journal of Physics: Conf. Series **1115**, 052010 (2018).

4 K. Shunkeyev, N. Zhanturina, L. Myasnikova, Z. Aimaganbetova, A. Barmina, Sh. Sagymbaeva and D. Sergeyev, Low temperature physics **42**, 580-583 (2016).

5 Y. Toyozawa, J. of Luminescence **12/13**, 13-21 (1976).

6 M.S. Mathews, B.T. Amaechi, K. Ramalingam, R.A. Ccahuana-Vasquez, I.P. Chedjieu, A.C. Mackey and R.L. Karlinsey, Archives of oral biology **57**, 525-530 (2012).

7 R.L. Whetten, Acc. Chem. Rev. **26**, 49-56 (1993)

8 R.D. Beck, P.St. John, M.L. Homer and R.L. Whetten, Chemical physical letters **187**, 122-128 (1991).

9 P.M.St. John, R.D. Beck and R.L. Whetten, Phys. Rev. Lett. **69**, 1467-1470 (1992).

10 J. Lumeau, K. Chamma, L. Glebova and L. Glebov, Journal of Non-Crystalline Solids **405**, 188–195 (2014).

11 I.S. Messaoudi, A. Zaoui and M. Ferhat, Phys. Status Solidi **B**, 1-6 (2014).

12 B.P. Mamula, B. Kuzmanović, M.M. Ilić, N. Ivanović and N. Novaković, Physica B: Condensed Matter **545**, 146-151 (2018).

13 Cui He, Cui-E Hu, Tian Zhang, Yuan-Yuan Qi and Xiang-Rong Chen, Solid State Communications **254**, 31-36 (2017).

14 Ting Liang, Wen-Qi Chen, Cui-E. Hu, Xiang-Rong Chen and Qi-Feng Chen, Solid State Communications **272**, 28-32 (2018).

15 B.P. Chandra, V.K. Chandra, Piyush Jha, R.P. Patel and R.N. Baghel, Radiation Measurements **78**, 9-16 (2015).

16 B.P. Chandra, Journal of Luminescence **128**, 1217–1224 (2008).

17 W. Kucharczyk, Journal of Physics and Chemistry of Solids **50(7)**, 709-712 (1989).

18 L. Bryukvina, N. Ivanov and S. Nebogin, Journal of Physics and Chemistry of Solids **120**, 133-139 (2018).

19 R. Pandey, X. Yang, J.M. Vail and J. Zuo, Solid State Communications **81(7)**, 549-552 (1992).

20 U. Landman, D. Scharf and J. Jortner, Physical review letters **54 (16)**, 1860-1863, (1985).

21 J. Hoya, J.I. Laborde, D. Richard and M. Rentería, Computational Materials Science **139**, 1-7 (2017).

22 D. Kong, C. Dong, X. Wei, C. Man, X. Lei, F. Mao and X. Li, Electrochimica Acta **292**, 817-827 (2018).

23 K.A. Jackson, Advances in Atomic, Molecular, and Optical Physics **64**, 15-27 (2015).

24 Myasnikova, A. Mysovskya, A. Paklin and A. Shalaev, Chemical Physics Letters **633**, 218-22, (2015).